

## Isovector $M2$ state observed in the $^{14}\text{C}(\pi^-, \gamma)$ reaction

Helmut W. Baer

*Los Alamos National Laboratory, University of California, Los Alamos, New Mexico 85745*

J. A. Bistirlich and K. M. Crowe

*Lawrence Berkeley Laboratory, University of California, Berkeley, California 94720*

W. Dahme

*Sektion Physik, Universität München, D-8046 Garching, Federal Republic of Germany*

C. Joseph and J. P. Perroud

*Institut de Physique Nucléaire, Université de Lausanne, CH-1015 Lausanne, Switzerland*

M. Lebrun,\* C. J. Martoff,† U. Straumann, and P. Truöl

*Physik-Institut, Universität Zürich, CH-8001 Zürich, Switzerland*

(Received 17 February 1983)

The photon spectrum of the pion capture reaction  $^{14}\text{C}(\pi^-, \gamma)^{14}\text{B}$  was measured with a resolution of 0.9 MeV full width at half maximum. A single strong transition is observed with  $\gamma$ -ray energy  $115.70 \pm 0.17$  MeV, corresponding to a state in  $^{14}\text{B}$  at  $2.15 \pm 0.17$ -MeV excitation. Comparisons with previous experiments and theoretical calculations identify this as the second  $T=2, 2^-$  state in mass-14 nuclei. The single strong transition has a measured branching ratio  $(11.1 \pm 3.0) \times 10^{-4}$ , which equals one-fifth of the shell-model prediction. The total radiative capture branching ratio is  $0.68 \pm 0.16\%$ , which is a factor of 2 to 3 smaller than for other  $1-p$ -shell nuclei.

NUCLEAR REACTIONS  $^{14}\text{C}(\pi^-, \gamma)^{14}\text{B}$  ( $E_x < 10$  MeV),  $T_\pi = 0$  MeV; measured photon spectra with pair spectrometer, compared with shell-model calculations.

### I. INTRODUCTION

We present here the results of our study on the reaction  $^{14}\text{C}(\pi^-, \gamma)$  with stopped pions. These measurements were motivated, in general, by the desire to have complete  $(\pi^-, \gamma)$  data on nuclei of the  $1p$  shell and the lower  $s-d$  shell to establish the pertaining nuclear structure systematics. With the completion of the present study all possible targets with  $A \leq 20$  will have been measured. The  $(\pi^-, \gamma)$  reaction selectively excites  $1^-$  states having large spin-transfer amplitudes ( $\Delta S = 1$ ) relative to the target ground states, and having angular momenta  $J_f$  that differ from the target angular momentum  $J_i$  by one or two units. The former feature is due to the dominance of  $\vec{\sigma}$  terms in the transition operator. The latter restriction results from the low-momentum transfer, near  $120$  MeV/ $c$ , in radiative pion capture.

For even- $N$ , even- $Z$  nuclei such as  $^{14}\text{C}$ , previous experiments show that generally the important states are the unnatural parity  $1^+$  and  $2^-$  states. In only one nucleus,  $^{12}\text{C}$ , was a peak observed in the photon

spectrum associated with a natural parity excitation. This was the  $1^-$  state at  $23.2$  MeV in  $^{12}\text{C}$  (Refs. 5 and 6). Several  $1^-$  states are predicted<sup>7</sup> to have significant  $(\pi^-, \gamma)$  strength in  $^{14}\text{C}$ . Unlike  $^{12}\text{C}$ ,  $1^+$  states should not be seen, because  $^{14}\text{C}$  has filled  $1p_{1/2}$  and  $1p_{3/2}$  neutron shells. This eliminates the charge-exchange spin-flip transitions without orbital rearrangement. Also, calculations<sup>4</sup> for  $0^-$ ,  $3^-$ , and  $4^-$  states show that the transition strengths to such states are very weak. Thus the general expectation for the present study was extension of the systematics of  $1^-$  and  $2^-$  isovector states with large spin-transfer amplitudes.

A more specific goal is the study of  $T=2$  states in mass-14 nuclei. Using the measured mass<sup>8</sup> of  $^{14}\text{B}$  and estimated Coulomb displacement energies, one obtains for the excitation energy of the lowest  $T=2$  states in  $^{14}\text{C}$ ,  $^{14}\text{N}$ , and  $^{14}\text{O}$  the values  $22.2$ ,  $24.3$ , and  $22.2$  MeV, respectively. At these high excitation energies, states are difficult to study because they are generally broad and overlapping. This is especially true for low-spin states. Also, a definite isospin

identification is nearly impossible when the states are produced in these nuclei, because states of lower  $T$  exist in the same excitation region. In the  $^{14}\text{C}(\pi^-, \gamma)^{14}\text{B}$  reaction, only the  $T=2$  level spectrum is observed, as  $^{14}\text{B}$  has  $T_z=2$ . The mirror nucleus,  $^{14}\text{F}$ , is particle-unstable and not amenable to level studies. This leaves almost no choice but to study the  $T=2$  levels in  $^{14}\text{B}$ . Because the  $(\pi^-, \gamma)$  reaction at threshold has a well-understood transition operator, this reaction presents a relatively unique opportunity for study of the  $1^-$  and  $2^-$ ,  $T=2$  states.

The systematics of  $2^-$  states in nuclei near  $^{16}\text{O}$  are particularly interesting in view of recent calculations,<sup>9,10</sup> which show that their energetic positions are quite sensitive to the spin-isospin part of the effective particle-hole interaction. The short-range repulsion mediated by the Migdal-parameter  $g'$  influences the level energies of the five  $2^-$  states that arise from coupling of  $1p_{3/2}$ ,  $1p_{1/2}$  holes with  $2s_{1/2}$ ,  $1d_{5/2}$ , and  $1d_{3/2}$  particles. The  $B(M2)$  values for these transitions, which are not well-known even in  $^{16}\text{O}$ , appear to be significantly quenched. This may reflect<sup>11</sup> the presence of  $\Delta$ -hole components in the nuclear wave functions. The  $1p_{3/2}$ -hole members of the quintet of  $2^-$  states may be studied also in the carbon isotopes. Among these isotopes,  $^{14}\text{C}$  has the simplest configurations owing to the closed neutron shell. The existing  $(\pi^-, \gamma)$  data on  $^{12}\text{C}$  (Refs. 5 and 6),  $^{16}\text{O}$  (Ref. 12),  $^{18}\text{O}$  (Ref. 12), and  $^{20}\text{Ne}$  (Ref. 13) lend support to the expected quenching of transition strength. In all cases, the conventional shell-model calculations overestimate the strength for the prominent  $2^-$  transitions.

In recent studies of inelastic pion<sup>14</sup> and electron<sup>15</sup> scattering on  $^{14}\text{C}$ , the region of the excitation spectrum between 20 and 30 MeV was examined. In the  $^{14}\text{C}(\pi, \pi')$  measurements, no narrow, identifiable states were observed in this region. In the  $^{14}\text{C}(e, e')$  measurements<sup>15</sup> at  $180^\circ$  scattering, preliminary results indicate the existence of a narrow  $4^-$  state at 24.3 MeV. If this is a  $T=2$  state, its analog in  $^{14}\text{B}$  would be near 2-MeV excitation. We would not expect to see this state in our experiment because of its high  $J$  value.

A search for the analog of the  $2^-$  ground state of  $^{14}\text{B}$  in  $^{14}\text{C}$  was performed by Kline *et al.*<sup>16</sup> using  $180^\circ$  electron scattering. Although the state was not observed, the analysis of its nonobservation in terms of the interference of two dominant particle-hole ( $p$ - $h$ ) configurations is supported by our results as discussed in Sec. IV.

The  $^{14}\text{B}$  levels were studied previously<sup>8</sup> with the charge-exchange reaction  $^{14}\text{C}({}^7\text{Li}, {}^7\text{Be})^{14}\text{B}$  at  $T({}^7\text{Li})=52$  MeV. The interpretation of these data is somewhat complicated, because each level in  $^{14}\text{B}$  is observed twice, once through the  ${}^7\text{Be}$  ground state

and once through the  ${}^7\text{Be}$  (0.431 MeV) state. On the basis of the similarity to the corresponding  $^{12}\text{C}({}^7\text{Li}, {}^7\text{Be})^{12}\text{B}$  reaction, multiplets of levels associated with the  $p$ - $h$  excitations ( $1d_{5/2} 1p_{3/2}^{-1}$ ) coupled to  $J^\pi=4^-, 3^-$ , and  $2^-$  and ( $1s_{1/2} 1p_{3/2}^{-1}$ ) coupled to  $J^\pi=2^-$  and  $1^-$  were identified. This identification of the predominant shell-model configurations as well as of the accurate excitation energies ( $\leq 0.06$  MeV error) was quite valuable in giving a definite interpretation of our results. The comparisons together with shell-model calculations are discussed in Sec. III and IV.

## II. EXPERIMENTAL PROCEDURES

A pion beam of momentum 220 MeV/ $c$  and flux  $10^8 \text{ s}^{-1}$  was delivered to our target from the SIN- $\pi$  E1 channel. This beam is extracted at a  $0^\circ$  production angle from a Be pion-production target. The upstream portion of this channel is shared with the high-intensity muon channel. During our data-taking period the muon experiments were designated primary users and determined the tune of the common section. In parasitic mode we were not able to optimize the tune as required by the thin- and small-area  $^{14}\text{C}$  target. The beam we obtained had a momentum bite  $\Delta p/p$  of 4% and a beam spot size of 6 cm horizontal and 10 cm vertical (FWHM). Under these conditions 1.4% of the  $\pi^-$  flux passed through the 2 by 3 cm beam-defining counter positioned 1.2 cm upstream from the target. Of these only 6.8% stopped in the  $^{14}\text{C}$  content of the target. Figure 1 depicts the degrader and target geometry.

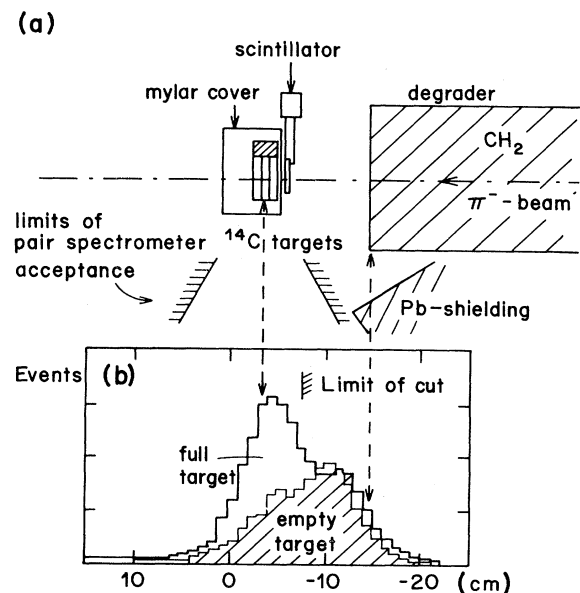


FIG. 1. (a) Experimental setup. (b) Reconstruction of the origin of the photon along the beam axis. Solid curve, target cell filled with  $^{14}\text{C}$ ; dashed line, empty target cell.

The  $^{14}\text{C}$  target consisted of four identical target cells stacked in contact with one another. The area of each target was 3 by 5 cm and the areal thickness was approximately  $0.1\text{ g/cm}^2$ . The cell design consisted of a stainless steel *U* frame to which was glued a 0.0025-cm stainless steel wraparound window. The  $^{14}\text{C}$  was packed into these cells through one end, which then was sealed by inserting a sintered steel plug. This target design was chosen for pion-scattering experiments with beam spot sizes less than 3 by 5 cm, and is not optimal for a pion-stopping experiment. The total mass of  $^{14}\text{C}$  plus  $^{12}\text{C}$  powder in the four targets was  $6.34 \pm 0.02\text{ g}$ . The  $^{14}\text{C}$  to  $^{12}\text{C}$  atom ratio as determined from five assays<sup>17</sup> was  $4.60 \pm 0.37$ . Thus the total  $^{14}\text{C}$  target thickness was  $356 \pm 5\text{ mg/cm}^2$  and the  $^{12}\text{C}$  thickness was  $66 \pm 5\text{ mg/cm}^2$ . The total stainless thickness in the eight windows was  $160 \pm 10\text{ mg/cm}^2$ . Identically constructed target frames containing  $^{12}\text{C}$  powder or no target material were used to measure backgrounds.

The photons were detected in a pair spectrometer whose technical description is given in Ref. 18. We used a 3% radiation-length gold converter that gave us a resolution at 129.4 MeV of 0.9 MeV (FWHM). The instrumental line shape was measured with the  $\pi^-p \rightarrow \gamma n$  reaction employing a liquid hydrogen target. The variation of spectrometer acceptance with photon energy was calculated by Monte Carlo simulation and checked with hydrogen runs. The  $\pi^-p \rightarrow \pi^0 n$  reaction produces a uniform photon spectrum between 55 and 83 MeV. The edges of this distribution and the 129.4-MeV line were used to check the spectrometer energy calibration to an accuracy of 0.1 MeV.

From the electron-positron trajectories the photon direction and its intersection with the target plane can be calculated. The measured resolution in the target position is 4 cm FWHM. The distribution of target interaction coordinates obtained in the present experiment is shown in Fig. 1(b). This distribution shows the presence of the target, which was physically placed at  $-2.0\text{ cm}$ . The presence of photons in the data arising from pions stopping near the downstream face of the degrader is also evident from Fig. 1(b). To eliminate most of these events, only  $\gamma$  rays with target coordinates in the range  $-7$  to  $20\text{ cm}$  were accepted in the spectra for final analysis. These events represent 0.47% of the total number of events written on tape. The total  $^{14}\text{C}$  data represent 3.5 d of running (taping) time.

The spectrum measured with the  $^{14}\text{C}$  target and surviving the target cuts is shown in Fig. 2(a). One sees in this spectrum contributions from  $^{14}\text{C}$ ,  $^{12}\text{C}$ ,  $^1\text{H}$ , and stainless steel. The spectra of scintillation material (a composite of hydrogen and  $^{12}\text{C}$ ), graphite

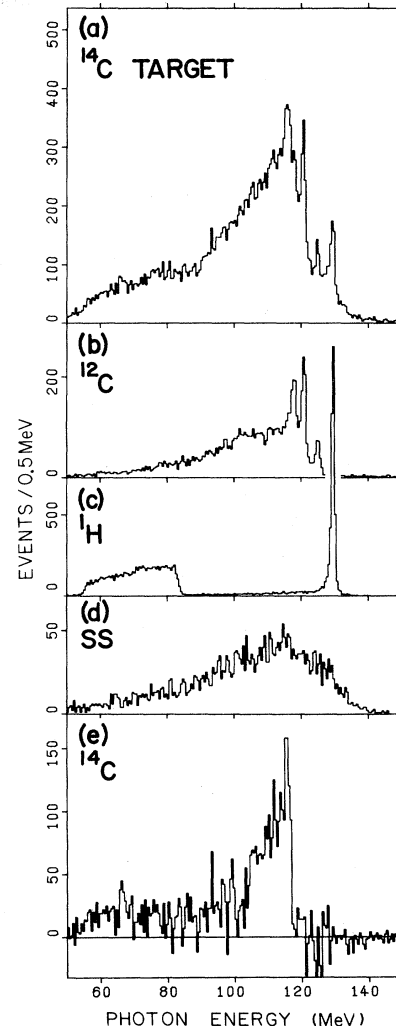


FIG. 2. Photon spectra from radiative pion capture measured in this experiment. (a)  $^{14}\text{C}$  target, raw spectrum. (b) Graphite target. (c) Hydrogen calibration spectrum. (d) Stainless steel. (e)  $^{14}\text{C}$  spectrum, remaining after subtraction of the  $^{12}\text{C}$ ,  $\text{H}_2$ , and steel contributions.

( $^{12}\text{C}$ ), and stainless steel were measured separately to give the data needed to subtract these components from the  $^{14}\text{C}$  target data. In addition, hydrogen spectra [Fig. 2(c)] were measured using a liquid hydrogen target. Figures 2(b) and (d) show the spectra for  $^{12}\text{C}$  and steel. The high  $Q$  value (21.15 MeV) for the  $^{14}\text{B}(\pi^-, \gamma)^{14}\text{C}$  reaction corresponds to the maximum kinematically possible photon energy of 117.84 MeV for pions bound in  $1s$  and  $2p$  atomic orbits.

Above 118 MeV we have only contributions from the impurities in the spectra. Each of these impurities has a distinguishing feature. Only the scintillator contains the  $\text{H}_2$  peak,  $^{12}\text{C}$  has two peaks at 125.0

and 120.4 MeV, and only steel can produce events between 130 MeV and the pion mass. A fit in the region above 118 MeV to a composite of these spectra with their relative yields left as free parameters therefore rapidly converges to a unique solution. Similar fits were made to the empty targets and those containing  $^{12}\text{C}$ . The results are summarized in Table I.

The branching ratios are computed from the number of incoming pions  $N_\pi$ , the stopping fraction  $f_\pi$ , the photon yield  $N_\gamma$ , and the acceptance of spectrometer<sup>18</sup>  $\eta = (2.66 \pm 0.10) \times 10^{-5}$  using the expression

$$B(\pi^-, \gamma) = N_\gamma (N_\pi f_\pi \eta)^{-1} f_\eta (f_a f_c)^{-1}, \quad (1)$$

where  $f_\eta$  is a correction factor to take into account the energy dependence of the spectrometer acceptance,  $f_a$  corrects for the absorption of photons on their way to the converter foil, and  $f_c$  is the fraction of good events lost in the tails of the target cuts. Only 18% of all events in the raw spectrum [Fig. 2(a)] are due to  $^{14}\text{C}$ ; therefore, the uncertainties in the measured branching ratios are somewhat larger than usual. The measured  $^{12}\text{C}$  branching ratios agree well with the averages of four previous measurements.<sup>4</sup>

### III. RESULTS AND COMPARISONS WITH OTHER EXPERIMENTS

Examination of the  $^{14}\text{C}$  spectrum [Fig. 2(e)] shows that three components appear to be present: (1) a sharp line near 116 MeV, (2) a featureless continuum between 80 and 105 MeV, and (3) some transition strength between 105 and 115 MeV, which may be in excess of the usual continuum shape and may be associated with unresolved nuclear states. Although the third component is not unambiguously evident from the data, the fact that shell-model calculations discussed below show considerable strength to  $1^-$  and  $2^-$  states in this region makes this representation of the data most probably correct. We note also that the line at 116 MeV appears broader than the instrumental line shape. This can be seen by comparing Figs. 2(a) and (c) with Fig. 2(e).

To determine the parameters of these components we used the pole-model spectrum<sup>1</sup> for the continuum and two Breit-Wigner resonance functions for the nuclear states. Both the positions and widths of these states were allowed to vary. The end point of the continuum was held fixed to correspond to the  $^{13}\text{B}(\text{g.s.}) + n$  vertex, which occurs 1.1 MeV above the  $^{14}\text{B}$  ground state. The results of this fit are

TABLE I. Quantities entering the computation of the measured branching ratios.

	Empty target	$^{12}\text{C}$ dummy target	$^{14}\text{C}$ target	Average
Pions <sup>a</sup>	$5.90 \times 10^{10}$	$2.06 \times 10^{10}$	$37.86 \times 10^{10}$	
Stopping fraction <sup>b</sup>	8.1%	16.8%	15.7%	
H <sub>2</sub> events <sup>c</sup>	$258 \pm 58$	$81 \pm 33$	$1224 \pm 148$	
$^{12}\text{C}$ events <sup>d</sup>	$787 \pm 154$	$980 \pm 109$	$8526 \pm 556$	
$^{12}\text{C}$ stopping fraction <sup>c</sup>	4.0%	13.1%	5.2%	
$^{12}\text{C}$ branching ratio <sup>e</sup>	$1.99 \pm 0.39\%$	$1.65 \pm 0.18\%$	$2.01 \pm 0.13\%$	$1.87 \pm 0.17\%$ <sup>f</sup>
Steel events <sup>d</sup>	$1143 \pm 187$	$341 \pm 125$	$8069 \pm 760$	
Steel stopping fraction <sup>b</sup>	4.1%	3.7%	3.7%	
Steel branching ratio <sup>e</sup>	$2.11 \pm 0.35\%$	$2.04 \pm 0.75\%$	$2.59 \pm 0.24\%$	$2.41 \pm 0.19\%$
$^{14}\text{C}$ events			$3896 \pm 888$	
$^{14}\text{C}$ stopping fraction <sup>b</sup>			6.8%	
$^{14}\text{C}$ branching ratio <sup>e</sup>			$0.68 \pm 0.17\%$	

<sup>a</sup>Number of pions passing the scintillator in front of the target ( $N_\pi$  in text).

<sup>b</sup>Fraction of pions stopping in the target material ( $f_\pi$  in text).

<sup>c</sup> $^{12}\text{C}$  includes scintillator; for  $^{14}\text{C}$  a thin Mylar foil is also included.

<sup>d</sup>The events have been corrected for the energy dependence of the efficiency; the unfolding factors are 1.12 for  $^{12}\text{C}$ , 1.16 for steel, 1.09 for  $^{14}\text{C}$ , and 1.43 for H<sub>2</sub>.

<sup>e</sup>Corrections are made for 15% events lost in target cut and 2% of photons absorbed in the target.

<sup>f</sup>Previous measurements are  $1.84 \pm 0.08$ ,  $1.92 \pm 0.19$ ,  $1.6 \pm 0.1$ , and  $2.1 \pm 0.4\%$  (Ref. 4).

presented in Table II and in Fig. 3.

Our results for the two lowest  $2^-$  levels differ in several respects from the results obtained in the only previous study<sup>8</sup> of the  $^{14}\text{B}$  levels. We find the relative branching ratio of the ground state ( $2_1^-$ ) to the second  $2^-$  state ( $2_2^-$ ) to be less than 0.1. A value of 1.6 was obtained for the relative cross sections of the  $^{14}\text{C}(^7\text{Li},^7\text{Be})^{14}\text{B}$  reaction. We obtain an excitation energy of  $2.15 \pm 0.17$  MeV for the  $2_2^-$  level compared to  $1.82 \pm 0.06$  MeV in Ref. 8. Lastly, our fit to the data gives a level width of  $1.0 \pm 0.5$  MeV for the  $2_2^-$  state. No value of the width was given in Ref. 8, although an examination of the published spectrum indicates that there may be some level broadening.

These differences can be understood as follows. Due to the higher momentum transfer  $q = 1.6 \text{ fm}^{-1}$  of the  $^{14}\text{C}(^7\text{Li},^7\text{Be})^{14}\text{B}$  reaction, as compared to  $q = 0.6 \text{ fm}^{-1}$  of the  $^{14}\text{C}(\pi^-, \gamma)^{14}\text{B}$  reaction, higher spin states are produced in the former reaction. Thus the strongest state, near 2-MeV excitation, seen in the  $^{14}\text{C}(^7\text{Li},^7\text{Be})^{14}\text{B}$  spectrum was identified as a  $4^-$  state at a measured energy of  $2.08 \pm 0.05$  MeV; a value of 3.8 was given for a cross-section ratio relative to the  $2_1^-$  state. The effect of having the  $4^-$  and  $2_2^-$  states close in energy, and of doubly observing each level in the  $(^7\text{Li},^7\text{Be})$  reaction (separated by 0.471 MeV), produces a broad unresolved structure near 2-MeV excitation. This makes the determination of the  $2_2^-$ -state energy and width quite uncertain. In the  $(\pi^-, \gamma)$  reaction the  $4^-$  state is absent and the  $2_2^-$  state is the strongest state in the spectrum. Thus the accuracy of our energy and width measurement is dominated by the statistical error rather than the background fitting error, and therefore should be more accurate.

The  $^{14}\text{C}(^7\text{Li},^7\text{Be})^{14}\text{B}$  data would seem to provide an upper limit on the width of the  $2_2^-$  state. A value between 0.4 and 0.8 MeV is quite consistent with these data if one assumes that at least 30% of the

observed strength is due to the  $2_2^-$  state. This result and our value of  $1.0 \pm 0.5$  MeV place the most probable value of the width in the range 0.5 to 1.0 MeV. Considering the preliminary results of the  $^{14}\text{C}(e, e')$  experiment<sup>15</sup> where a level width  $\Gamma(4^-) < 0.3$  MeV is reported, one obtains a picture of this region of excitation showing a narrow  $4^-$  state overlapping a broad  $2^-$  state, both centered at an excitation energy of  $2.1 \pm 0.1$  MeV.

The one remaining difference between the two studies is the relative  $2_1^-/2_2^-$  strength. Most shell-model calculations, as discussed below, describe these states as mixtures of  $(2s_{1/2} 1p_{3/2}^{-1})$  and  $(1d_{5/2} 1p_{3/2}^{-1})$  configurations. The  $2_1^-$  state consists primarily of the former configuration; the  $2_2^-$  state, of the second configuration. The squares of the  $M2$  form factors<sup>16</sup> associated with these configurations peak near  $q = 2 \text{ fm}^{-1}$  and  $q = 0.8 \text{ fm}^{-1}$ , respectively. The ratio of form factors changes from 1:70 to 5:1 in going from  $q = 0.6 \text{ fm}^{-1}$  to  $q = 1.5 \text{ fm}^{-1}$ , respectively. These ratios, evaluated for electron scattering, show the tremendous sensitivity to  $q$  contained within these configurations ( $2s_{1/2}$  vs  $1d_{5/2}$ ). It is not unreasonable to expect this sensitivity to be responsible in part for the difference in the relative strengths seen in the  $(\pi^-, \gamma)$  and  $(^7\text{Li},^7\text{Be})$  reactions.

In Table III we compare results for the  $^{12}\text{C}(\pi^-, \gamma)^{12}\text{B}$  and  $^{14}\text{C}(\pi^-, \gamma)^{14}\text{B}$  reactions on the two lowest  $2^-$  states. For both nuclei the  $2_2^-$  state has a much larger  $(\pi^-, \gamma)$  branching ratio than the  $2_1^-$  state. For  $^{12}\text{C}$  the relative branching ratio is 30 to 1; for  $^{14}\text{C}$  the  $2_1^-$  state was not observed, but a lower limit of 10 to 1 is obtained for this ratio. The  $2_2^-$  states have a natural width of order 0.5 MeV in both  $^{12}\text{B}$  and  $^{14}\text{B}$ . Preliminary results from 180 electron scattering experiments<sup>15,22</sup> indicate that these states in  $^{12}\text{C}$  and  $^{14}\text{C}$  also have widths of order 0.5 MeV. They occur at  $19.4 \pm 0.1$  MeV and  $24.3 \pm 0.2$  MeV, respectively. The widths of the  $2_1^-$  states in  $^{12}\text{B}$  and

TABLE II. Results for the  $^{14}\text{C}(\pi^-, \gamma)$  reaction.

$E_\gamma$ (MeV)	$E_x(^{14}\text{B})$ (MeV)	Number of events	$J^\pi$	$\Gamma$ (MeV)	$B(\pi^-, \gamma)$ ( $10^{-4}$ )
117.85 <sup>a</sup>	0.0	$7^{+8.4}_-7$	$2^-$	0.0	$0.1^{+1.2}_{-0.1}$
$115.70 \pm 0.17$	2.15	$632 \pm 172$	$2^-$	$1.0 \pm 0.5$	$11.1 \pm 3.0^b$
$112.1 \pm 1.6$	6.7	$1223 \pm 612$	$(1^-, 2^-)$	$7.8 \pm 3.2$	$21.4 \pm 10.7^b$
$\leq 116.8$	$\geq 1.1$	$2034 \pm 615$		continuum <sup>c</sup>	$35.7 \pm 10.8^b$
Total		$3896 \pm 888$			$68.3 \pm 15.6^b$

<sup>a</sup>Kinematical value, assuming a mass excess of 23.657 MeV for  $^{14}\text{B}$  and a  $2p$ -shell atomic binding energy of 33 keV for the pion.

<sup>b</sup>Uncertainty in the fit, including the statistical errors from the background subtraction. A normalization error of 10% must be combined in quadrature to get the total error (see Table I).

<sup>c</sup>Pole model (discussed in Ref. 1) with  $\Delta = 22.1$  MeV, corresponding to the  $^{13}\text{B}(\text{g.s.}) + n$  vertex.

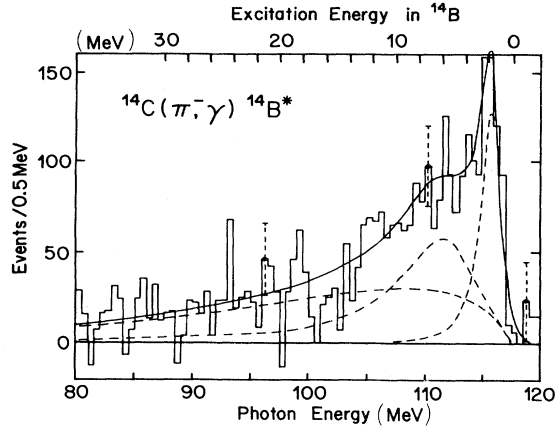


FIG. 3.  $^{14}\text{C}(\pi^-, \gamma)^{14}\text{B}^*$  photon spectrum compared to a fit to the spectrum. Solid curve, total spectrum; dashed curve, individual contributions. The statistical errors from the background subtraction do not vary significantly over the spectrum and are only shown for a few points.

$^{14}\text{B}$  are not measured in the  $(\pi^-, \gamma)$  experiments. In  $^{12}\text{C}$  the  $2_1^-$  state has a width  $0.4 \pm 0.1$  MeV and occurs at an energy of  $16.6 \pm 0.1$  MeV.<sup>22</sup> In  $^{14}\text{C}$  the  $2_1^-$  state is at  $22.1 \pm 0.2$  MeV and has a width of  $< 0.3$  MeV.<sup>15</sup> In  $^{12}\text{B}$  and  $^{14}\text{B}$ , the  $2_1^-$  states are particle-stable.

There is a further similarity between  $^{12}\text{C}$ ,  $^{14}\text{C}$ , and even  $^{13}\text{C}$ , which is quite remarkable. In both  $^{12}\text{C}$  and  $^{14}\text{C}$  the  $2_2^-$  state is nearly degenerate in energy with the lowest  $4^-$  state ( $4_1^-$ ) of the same isospin. In

$^{12}\text{C}$  the  $4_1^-$  state has an excitation energy  $19.59 \pm 0.04$  MeV (Ref. 22); in  $^{14}\text{C}$  it is at  $24.3 \pm 0.2$  MeV.<sup>15</sup> These values are within 0.2 MeV of the  $2_2^-$  energies given above. The near degeneracy of the  $2_2^-$  and  $4_1^-$  states in  $^{12}\text{C}$  was the cause of the oscillatory angular distribution in the  $^{12}\text{C}(e, e'\pi^+)^{12}\text{B}$  reaction measured by Min *et al.*,<sup>23</sup> where the two states were not resolved. A very similar oscillatory pattern was observed<sup>24</sup> for the  $^{13}\text{C}(e, e'\pi^+)^{13}\text{B}$  reaction for states near 21.5-MeV excitation, indicating that sizable  $M4$  and  $M2$  strength exists to unresolved  $T = \frac{3}{2}$  states in this region. This is supported by results of two other experiments.

A strong  $M4$  transition was observed in  $180^\circ$  electron scattering on  $^{13}\text{C}$  by Hicks *et al.*<sup>25</sup> to a state at  $21.5 \pm 0.1$  MeV. It has a width of  $\Gamma = 0.34 \pm 0.04$  MeV. In the same experiment two additional states were observed in the lower- $q$  data ( $q \approx 1 \text{ fm}^{-1}$ ) near 22.0 and 22.7 MeV. In the  $^{13}\text{C}(\pi^-, \gamma)$  study<sup>26</sup> two peaks in the photon spectrum were identified with states in  $^{13}\text{C}$  at 21.6 and 22.7 MeV. Most probably the observed peaks correspond to isovector  $M2$  transitions in  $^{13}\text{C}$ ; they are identified as  $\frac{3}{2}^+$  and  $\frac{5}{2}^+$  states, respectively, in Ref. 26 (the ground state is  $\frac{1}{2}^-$ ). The  $M4$  transition in  $^{13}\text{C}$  was tentatively identified<sup>25</sup> with a  $\frac{9}{2}^+$  state at 21.5 MeV. These three states in  $^{13}\text{C}$  are believed to correspond in large measure to  $(1d_{5/2} 1p_{3/2}^{-1})$ ,  $T=1$ ,  $p$ - $h$  excitations on the  $^{13}\text{C}$  ground state, giving  $\frac{3}{2}^+$  and  $\frac{5}{2}^+$  states when the  $p$ - $h$  excitation is coupled to  $2^-$ , and then coupled to the  $\frac{1}{2}^-$  ground state. The state with  $\frac{9}{2}^+$  is produced when the  $p$ - $h$  excitation couples to  $4^-$ . The

TABLE III. Comparison of  $(\pi^-, \gamma)$  branching ratios for the lowest two  $2^-$  states  $^{12}\text{B}$  and  $^{14}\text{B}$ .

State	$E_x(B)$ (MeV)	$E_x(C)$ (MeV)	$B(\pi^-, \gamma)$ ( $10^{-4}$ )	$\Gamma$ (MeV)	$B(\text{theory})$ ( $10^{-4}$ )
$^{12}\text{C}, 2_1^-, T=1$	1.67 <sup>a</sup>	16.58 <sup>b</sup>	$0.50 \pm 0.18^a$	$0.4 \pm 0.1^c$	1 <sup>d</sup> 0.25 <sup>e</sup>
$^{14}\text{C}, 2_1^-, T=2$	0.0	22.1 <sup>f</sup>	$0.1(-0.1, +1.2)^g$		9 <sup>h</sup> $\approx 0^h$
$^{12}\text{C}, 2_2^-, T=1$	4.37 <sup>a</sup>	19.35 <sup>b</sup>	$18.32 \pm 0.60^a$	$0.89 \pm 0.07^a$	50 <sup>d</sup> 60 <sup>e</sup>
$^{12}\text{C}, 2_2^-, T=1$			$18.5 \pm 1.9^i$	$0.45 \pm 0.12^i$	
$^{12}\text{C}, 2_2^-, T=1$			$16.4 \pm 1.7^g$	$0.49 \pm 0.10^g$	
$^{14}\text{C}, 2_2^-, T=2$	2.1 <sup>g</sup>	24.2 <sup>j</sup>	$11.1 \pm 3.0^g$	$1.04 \pm 0.48^g$	53 <sup>h</sup> 64 <sup>h</sup>

<sup>a</sup>Reference 6.

<sup>b</sup>Reference 22.

<sup>c</sup>Width of 16.58-MeV state in  $^{12}\text{C}$ ; Ref. 22.

<sup>d</sup>Reference 20, Tamm-Dancoff approximation.

<sup>e</sup>Reference 21, continuum shell model.

<sup>f</sup>Reference 15.

<sup>g</sup>This experiment.

<sup>h</sup>Reference 7; first column, Cohen-Kurath (Ref. 34) plus Gillet-COP (Ref. 35); second column, Cohen-Kurath plus Millener-Kurath (Ref. 33).

<sup>i</sup>Reference 19.

<sup>j</sup>Assuming a 2.1-MeV energy spacing between the  $2^-$  states in  $^{14}\text{C}$ .

( $2s_{1/2} 1p_{3/2}^{-1}$ ),  $T=1, 2_1^-$  excitation on the  $^{13}\text{C}$  ground state produces  $\frac{3}{2}^+$  and  $\frac{5}{2}^+$  states in  $^{13}\text{C}$  at a lower energy. Candidates for these states are observed (weakly) at 18.6 MeV in the  $^{13}\text{C}(\pi^-, \gamma)^{13}\text{B}$  experiment.<sup>26</sup>

In summary, we see that the  $(\pi^-, \gamma)$  data show a strikingly similar pattern in the  $2_1^-$  and  $2_2^-$  isovector excitations built on the  $^{12}\text{C}$ ,  $^{13}\text{C}$ , and  $^{14}\text{C}$  ground states. This pattern is corroborated by the  $180^\circ$  electron scattering data and the  $(e, e'\pi)$  data. The latter studies further show that in all three nuclei the lowest  $4_1^-$  isovector state is nearly degenerate in energy with the  $2_2^-$  excitation.

In regard to the  $2_2^-$  and  $4_1^-$  states in  $^{12}\text{C}$ , it is interesting to note that recent pion inelastic scattering experiments on  $^{12}\text{C}$  show<sup>27</sup> that there is considerable isospin mixing of levels near 20-MeV excitation. Preliminary analyses<sup>27</sup> indicate that there are two  $4^-$  states at 19.3 and 19.7 MeV and that each of these states consists of nearly equal components on  $T=0$  and  $T=1$  configurations [predominantly ( $1d_{5/2} 1p_{3/2}^{-1}$ )]. The pion data also give an indication<sup>27</sup> that the  $2^-$  states are isospin mixed, but to a lesser degree. In the preliminary analysis,<sup>27</sup>  $2^-$  states at energies 18.3 and 19.3 MeV were obtained. The latter state is thought to be mostly  $T=1$ , the former mostly  $T=0$ . Isospin admixtures of 30% ( $T=1$  into the 18.3-MeV state,  $T=0$  into the 19.3-MeV state) are consistent with the data. These results from the pion experiments have not yet been fully reconciled with the  $2_2^-$  and  $4_1^-$  states identified in electron scattering. On the basis of excitation energy, one would associate the 19.7-MeV,  $4^-$  state and the 19.3-MeV,  $2^-$  state with the states identified in the above discussion of electron scattering. In the  $^{12}\text{C}(\pi^-, \gamma)$  reaction, only the  $T=1$  components of these isospin mixed states are observed.

In both the  $^{12}\text{C}(\pi^-, \gamma)$  and  $^{14}\text{C}(\pi^-, \gamma)$  photon spectra there is transition strength to states above the  $2_2^-$  state. For  $^{12}\text{C}$  there is a peak in the spectrum<sup>6</sup> corresponding approximately to 8-MeV excitation in  $^{12}\text{B}$  (23 MeV in  $^{12}\text{C}$ ). This peak is broader than the instrumental line width and has been interpreted<sup>6</sup> as transition strength to unresolved  $1^-$  and  $2^-$  states. In the  $^{14}\text{C}(\pi^-, \gamma)$  spectrum of Fig. 3 one sees transition strength to states above the  $2_2^-$  state, but no isolated peak. Kissener and Eramzhyan<sup>7</sup> predict  $(\pi^-, \gamma)$  strength in this region to two  $1^-$  states, predominantly due to ( $1d_{5/2} 1p_{3/2}^{-1}$ ) and ( $1d_{3/2} 1p_{3/2}^{-1}$ ) excitations, and to a  $2^-$  state with a predominant ( $1d_{3/2} 1p_{3/2}^{-1}$ ) configuration. These states are predicted to lie between 3- and 7-MeV excitation in  $^{14}\text{B}$ . We cannot resolve these states, but consider it quite likely that they constitute the major features of the transition strength to this region. Our fit of a broad Breit-Wigner resonance function

for this transition strength resulted (Table II) in a branching ratio  $(21.4 \pm 10.7) \times 10^{-4}$ , which is approximately twice that of the  $2_2^-$  state  $(11.1 \pm 3.0) \times 10^{-4}$ . These numbers are consistent with the theoretical ratio<sup>7</sup> 1.2 for the strengths of these two components. The full theoretical spectrum is compared with the data in Sec. IV.

In Fig. 4 we give the  $^{14}\text{B}$ - $^{14}\text{C}$  level scheme for  $T=2$  levels as presently known. It is based on Refs. 8 and 15 and on this experiment. The  $^{14}\text{C}(\pi^-, \gamma)$  data establish the presence of the  $2_2^-$  state at 2.1 MeV and give a first measurement of its width. Also, our data are highly suggestive of the existence of  $2^-$  and  $1^-$  states in the 5- to 7-MeV region of  $^{14}\text{B}$ . The values of 5 and 7 MeV shown in Fig. 4 are theoretical values<sup>7</sup> for the  $2_3^-$  state and the  $1^-$  state with the largest  $(\pi^-, \gamma)$  transition rate, respectively.

#### IV. SHELL-MODEL ANALYSIS OF THE $^{12}\text{C}$ AND $^{14}\text{C}(\pi^-, \gamma)$ BRANCHING RATIOS FOR THE LOWEST $2^-$ STATES

The negative parity states at low-excitation energy in  $^{12}\text{B}$  and  $^{14}\text{C}$  are described by nearly identical particle-hole combinations. The filling of the  $1p_{1/2}$  neutron shell in  $^{14}\text{C}$  does have, however, two immediate consequences. The  $1^+$  excitation ( $1p_{1/2} 1p_{3/2}^{-1}$ ) giving the well-known 15.1 MeV in  $^{12}\text{C}$  is absent in  $^{14}\text{C}$ . Also, the transitions from the  $1s_{1/2}$  core to the  $1p_{1/2}$  shell are blocked by the Pauli exclusion principle. Such transitions would be expected<sup>28</sup> around 30 MeV in  $^{12}\text{C}$  and at a somewhat higher energy in  $^{14}\text{C}$ . The absence of ( $1p_{1/2} 1s_{1/2}^{-1}$ ) excitations in  $^{14}\text{C}$  may explain why the photon spectrum looks emptier at lower energies than for  $^{12}\text{C}$ ,

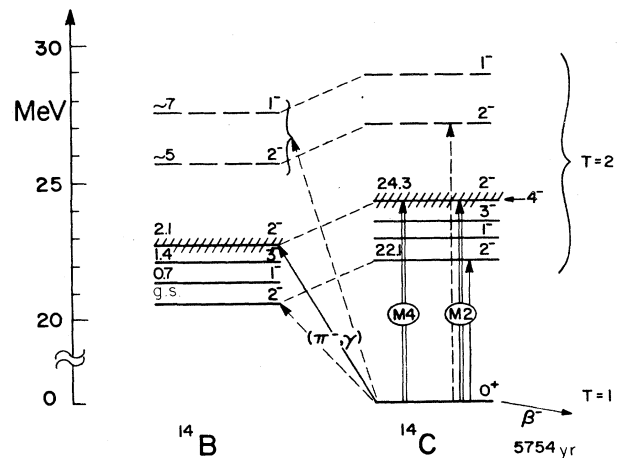


FIG. 4.  $^{14}\text{C}$ - $^{14}\text{B}$  level diagram showing the  $T=2$  states presently known, and transitions of interest to the present study.

and why the total branching for  $^{14}\text{C}$  is only one third of that for  $^{12}\text{C}$ . Although there are these differences between  $^{12}\text{C}$  and  $^{14}\text{C}$ , we do not expect them to significantly affect the relative branching ratios to the  $1^-$  and  $2^-$  states in the two nuclei which we now discuss.

The  $1^-$  and  $2^-$  states can be formed from  $1p_{3/2}^{-1}$  hole and  $2s_{1/2}$ ,  $1d_{5/2}$ , and  $1d_{3/2}$  particle

$$\begin{aligned} |2_1^-; 18.8 \text{ MeV}\rangle &= 0.94 |2s_{1/2} 1p_{3/2}^{-1}\rangle - 0.34 |1d_{5/2} 1p_{3/2}^{-1}\rangle - 0.02 |1d_{3/2} 1p_{3/2}^{-1}\rangle, \\ |2_2^-; 20.6 \text{ MeV}\rangle &= 0.34 |2s_{1/2} 1p_{3/2}^{-1}\rangle + 0.93 |1d_{5/2} 1p_{3/2}^{-1}\rangle - 0.14 |1d_{3/2} 1p_{3/2}^{-1}\rangle, \\ |2_3^-; 23.8 \text{ MeV}\rangle &= 0.07 |2s_{1/2} 1p_{3/2}^{-1}\rangle + 0.12 |1d_{5/2} 1p_{3/2}^{-1}\rangle + 0.99 |1d_{3/2} 1p_{3/2}^{-1}\rangle. \end{aligned} \quad (2)$$

Because the  $2s_{1/2}$  and  $1d_{5/2}$  single-particle energies differ by only 0.9 MeV, the  $2_1^-$  and  $2_2^-$  states are mixed to two nearly orthogonal combinations of these configurations. The experimental energies for these three states are<sup>22</sup>  $16.6 \pm 0.1$ ,  $19.4 \pm 0.1$ , and  $22.8 \pm 0.1$  MeV, respectively. (Only a tentative  $2^-$  assignment<sup>25</sup> exists for the 22.8-MeV state.) In  $^{12}\text{B}$  the states occur at 2.6, 4.4, and 8.8 MeV, respectively.

It is straightforward to obtain the  $(\pi^-, \gamma)$  branching ratios for  $2^-$  states with the above configurations. Neglecting  $1s$  capture and smaller matrix elements, one can use the expressions given by Ohtsuka<sup>29</sup> and Perrenoud<sup>30</sup> to obtain the transition rate

$$\begin{aligned} \lambda_\gamma(0^+ \rightarrow 2^-) &= \frac{k}{m_\pi} \frac{(1 + m_\pi/m_n)^2}{1 + k/M_A} \frac{4\pi}{3} a_\pi^{-5} \frac{C_{2p}}{24} \left[ \frac{A}{k} \right]^2 |\langle 2^- | [\vec{\sigma} \times \hat{Y}_1]^2 t^+ | 0^+ \rangle|^2 \\ &\times \frac{2}{3} |\langle nlj | -krj_0 - \frac{1}{10} krj_2 + \frac{9}{10} (\beta - \frac{2}{3}\gamma) j_1 | 1p_{3/2}^3 \rangle|^2 \\ &+ \frac{24}{25} |\langle nlj | krj_2 + (\beta + \gamma) j_1 | 1p_{3/2}^3 \rangle|^2 + \frac{3}{10} |\langle nlj | -krj_2 + (2\gamma - \beta) j_1 | 1p_{3/2}^3 \rangle|^2. \end{aligned} \quad (3)$$

Here  $A, \beta = (B/A)k^2$  and  $\gamma = (C/A)k^2$  are the coefficients of the elementary photopion production amplitude, having values<sup>1</sup>  $A = -32.6 \times 10^{-3} m_\pi^{-3}$ ,  $B = 7 \times 10^{-3} m_\pi^{-3}$ , and  $C = -27 \times 10^{-3} m_\pi^{-3}$ .  $M$ ,  $M_A$ , and  $a_\pi$  denote the nucleon mass, nuclear mass, and the pionic Bohr radius, respectively. The  $0^+$  initial nuclear state is assumed to consist of the  $(1p_{3/2})^4$  proton configuration, and the  $2^-$  final state is assumed to be a  $T=1$   $p$ - $h$  excitation with configuration  $(nlj)(p_{3/2}^{-1})$  coupled to  $2^-$ .

We can evaluate the radial integrals containing the spherical Bessel function of argument  $kr$  using the expressions given by deForest and Walecka.<sup>31</sup> The wave numbers are  $k=116$  MeV for  $^{14}\text{C}$  and 120 MeV for  $^{12}\text{C}$ . The single-particle wave functions are harmonic oscillator eigenstates with radius parameter  $b=1.88$ . These functions for  $b=1.88$  are sharply peaked near the nuclear surface ( $r \cong 2.5$  fm). Therefore, we have replaced the distorted pion wave func-

tion, which appears in the integrals, by a distortion factor  $C_{1p}$  (evaluated at  $r=2.5$  fm,  $C_{2p}=1.41$ ) multiplying a hydrogenic wave function. The latter varies linearly with  $r$  near the origin.

The measured branching ratios  $B(\pi^-, \gamma)$  are ratios  $\lambda_\gamma/\Gamma_{2p}$  of the  $(\pi^-, \gamma)$  transition rate as given by Eq. (3) and the total level width of the  $2p$ -pionic level. For the carbon isotopes the  $1s$ -state capture probability is only a few percent.<sup>1</sup> The measured<sup>32</sup>  $2p$ -level widths are

$$\Gamma_{2p}(^{12}\text{C}) = 1.17 \pm 0.11 \text{ eV}$$

and

$$\Gamma_{2p}(^{13}\text{C}) = 0.97 \pm 0.10 \text{ eV}.$$

Because the  $^{14}\text{C}$  width has not been measured, we use the  $^{13}\text{C}$  value for the present analysis.

Using Eq. (3) and the above  $2p$ -level width, we obtain  $(\pi^-, \gamma)$  branching ratios

$$B(0^+ \rightarrow 2^-) = 18 \times 10^{-4} R_{21}^2(^{14}\text{C}); 17 \times 10^{-4} R_{21}^2(^{12}\text{C}) \quad (4a)$$

for the  $1p \rightarrow 2s$  single-particle transition, and

$$B(0^+ \rightarrow 2^-) = 83 \times 10^{-4} R_{21}^2(^{14}\text{C}); 70 \times 10^{-4} R_{21}^2(^{12}\text{C}) \quad (4b)$$

for  $1p \rightarrow 1d$  transitions. The spin-multipole operators  $R_{LJ} = \langle [\hat{\sigma} \cdot Y_L]^J \rangle$  have the values<sup>29</sup>  $(5/2\pi)^{1/2}$ ,  $(21/10\pi)^{1/2}$ , and  $(2/5\pi)^{1/2}$  for the single-particle states  $2s_{1/2}$ ,  $1d_{5/2}$ , and  $1d_{3/2}$ , respectively. If we include  $1s$  capture, the factors in Eq. (4a) change by less than 10%. The higher spin multipoles  $R_{32}$  and  $R_{33}$  appear with coefficients which are typically 5% to 15% of those of  $R_{21}$  and thus do not change the single-particle estimates significantly (except for the  $1d_{3/2}$  case, where  $R_{33}$  contributes 40%). In particular, the only non-spin-flip term, arising from  $\langle [Y_3] \rangle$ , contributes less than 1%. Therefore our reaction is seen to be sensitive only to spin-density matrix elements. Inserting the above values of  $R_{21}$ , we obtain for the branching ratios

$$(2s_{1/2} 1p_{3/2}^{-1}): 14 \times 10^{-4} (^{14}\text{C}) 14 \times 10^{-4} (^{12}\text{C}), \quad (5a)$$

$$(1d_{5/2} 1p_{3/2}^{-1}): 55 \times 10^{-4} (^{14}\text{C}) 47 \times 10^{-4} (^{12}\text{C}), \quad (5b)$$

$$(1d_{3/2} 1p_{3/2}^{-1}): 11 \times 10^{-4} (^{14}\text{C}) 9 \times 10^{-4} (^{12}\text{C}). \quad (5c)$$

We see that the  $(1d_{5/2} 1p_{3/2}^{-1})$  configuration leads to the strongest  $(\pi^-, \gamma)$  transitions. Because this configuration dominates the  $2_2^-$  state in  $^{12}\text{C}$  and  $^{14}\text{C}$ , this state produces the large peak in the photon spectrum in each case.

Note that the above values are not too different from the complete calculations (Table III) of Kissener and Eramzhyan<sup>7</sup> using Cohen-Kurath plus Gillet-COP matrix elements or the Millener-Kurath  $p$ - $h$  matrix elements. Even a continuum shell-model calculation, as is available<sup>21</sup> for  $^{12}\text{C}$ , does not alter the results dramatically.

In view of the small values for the  $(1d_{3/2} 1p_{3/2}^{-1})$  amplitudes contained in the  $2_1^-$  and  $2_2^-$  states [Eq. (2)], we analyzed the  $^{12}\text{C}$  and  $^{14}\text{C}(\pi^-, \gamma)$  branching ratios assuming wave functions

$$|2_1^- \rangle = \cos\phi |2s_{1/2} 1p_{3/2}^{-1} \rangle - \sin\phi |1d_{5/2} 1p_{3/2}^{-1} \rangle, \quad (6)$$

$$|2_2^- \rangle = \sin\phi |2s_{1/2} 1p_{3/2}^{-1} \rangle + \cos\phi |1d_{5/2} 1p_{3/2}^{-1} \rangle.$$

We find that the minimum value for the ratio  $B(2_1^-)/B(2_2^-) = 0.22$  is obtained with  $\phi = 15^\circ$ . Inclusion of  $1s$  capture reduces this value to 0.18. If the harmonic oscillator parameter is changed to 1.64 fm (an alternative value used by Donnelly<sup>28</sup>), the minimum occurs at  $\phi = 20^\circ$  with a ratio of 0.14. These values of  $\phi$  agree with the theoretical values of Donnelly,<sup>28</sup> but do not agree with the  $^{12}\text{C}$  and  $^{14}\text{C}$  experimental ratios of  $B(2_1^-)/B(2_2^-)$ . The calcula-

tions of Kissener and Eramzhyan<sup>7</sup> indicate a possible way out of this dilemma. Use of the Millener-Kurath<sup>33</sup> interaction, which contains noncentral terms and generally improves the agreement between the predicted and experimental positions of the unnatural parity states in the  $1p$  shell, leads to a reduced transition strength to the  $2_1^-$  state that is consistent with the experimental upper limit. The sum of the two branching ratios is independent of the mixing angle and can be used to determine the quenching factors ( $r_q$ ) for the matrix elements. We find  $r_q = 0.40 \pm 0.05$  for  $^{14}\text{C}$  and  $r_q = 0.56 \pm 0.02$  for  $^{12}\text{C}$ . Similar quenching factors are needed for the complete shell-model results. This reduction was also noted by Donnelly<sup>28</sup> in his comparison with inelastic electron scattering data for the  $2_2^-$  level in  $^{12}\text{C}$ .

In Fig. 5 we compare our spectrum to the full shell-model results. The theoretical branching ratios have been reduced by a factor of 5 to match the strongest  $2^-$  transition. The theoretical spectra are convoluted with the instrumental resolution and energy-dependent acceptance. In addition, we assumed a natural line width of 1 MeV for all theoretical levels except for the  $^{14}\text{B}$  ground state. The overall representation of the data is seen to be quite satisfactory.

## V. SUMMARY AND CONCLUSIONS

The present study on  $^{14}\text{C}$  has completed the  $(\pi^-, \gamma)$  reaction systematics of isovector  $M2$  excitations in the carbon isotopes, and has confirmed the trends for  $2^-$  state excitation found throughout the  $1p$  shell and lower  $2s$ - $1d$  shell. For the carbon iso-

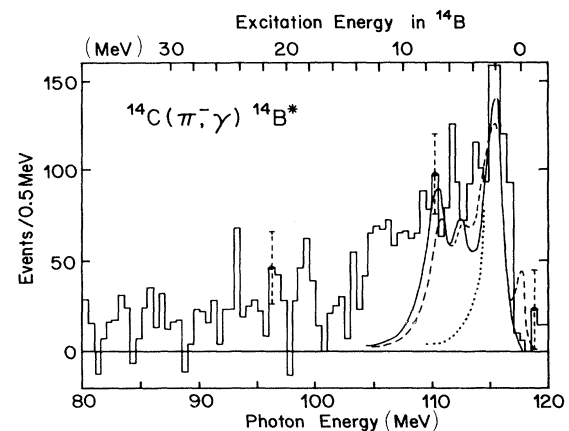


FIG. 5. The  $^{14}\text{C}(\pi^-, \gamma)^{14}\text{B}$  photon spectrum compared to the shell-model calculations of Ref. 7. Solid curve, Cohen-Kurath plus Gillet-COP  $p$ - $h$  interaction; dashed curve, Cohen-Kurath plus Millener-Kurath  $p$ - $h$  interaction; dotted curve, contribution of the  $2_2^-$  state predicted at  $E_x(^{14}\text{B}) = 1.8$  MeV.

topes we see the second  $2^-$  excitation, predominantly ( $1d_{5/2} 1p_{3/2}^{-1}$ ), carrying most of the ( $\pi^-, \gamma$ ) strength. The lowest energy  $2^-$  excitation, predominantly ( $2s_{1/2} p_{3/2}^{-1}$ ), is much weaker. The highest energy  $2^-$  excitation, predominantly ( $1d_{3/2} p_{3/2}^{-1}$ ), is not as clearly distinguishable in the  $^{14}\text{C}$  ( $\pi^-, \gamma$ ) spectrum as it is in those of  $^{12}\text{C}$  and  $^{13}\text{C}$ . A further feature of the "giant isovector  $M2$ " state is that it is broadened, both as the parent state in  $^{12}\text{B}$  or  $^{14}\text{B}$  and in the target nucleus  $^{12}\text{C}$  or  $^{14}\text{C}$ . Its width is approximately 0.5 MeV. Shell-model analyses of the transition rates to this state in  $^{12}\text{C}$ ,  $^{13}\text{C}$ , and  $^{14}\text{C}$  overestimate the measured rates by factors of 2 to 5.

The latter feature is a trend of the ( $\pi^-, \gamma$ ) data that exists for all cases investigated so far. In addition to the three carbon isotopes, the quenched  $M2$  strength is observed in  $^{16}\text{O}$  and  $^{18}\text{O}$  (Ref. 12) and  $^{20}\text{Ne}$  (Ref. 13). In these cases the observed strength misses the predicted values by a factor of approxi-

mately 2. Only for  $^{16}\text{O}$  have attempts been made to account for the missing strength. The inclusion of  $2h\omega$  admixtures into the ground states typically removes one half of the discrepancy. Higher-order admixtures into the final states have only a small effect. Thus one is led to consider more exotic mechanisms like  $\Delta$ - $h$  admixtures to account for the missing strength. Recently such investigations have begun.<sup>9-11</sup> However, before firm conclusions are possible, extensive systematics must be compiled. The present study on  $^{14}\text{C}$ , which has located the "isovector  $M2$  resonance" in this important single closed-shell nucleus, is a step in this direction.

This work was supported by the Swiss Institute of Nuclear Research (SIN), the Swiss National Science Foundation, the German "Bundesministerium für Forschung und Technologie," and the Division of Nuclear Physics of the U.S. Department of Energy.

\*Present address: Institut de Physique Corpusculaire, Université Catholique de Louvain, Louvain-la-Neuve, 1348 Belgium.

†Present address: Department of Physics, Stanford University, Stanford, CA 94303.

<sup>1</sup>H. Baer, K. M. Crowe, and P. Truöl, *Adv. Nucl. Phys.* **9**, 177 (1977).

<sup>2</sup>J. P. Perroud, Lecture presented at the Seminar on Electromagnetic Interactions of Nuclei at Low and Medium Energies, Moscow, 1981 (unpublished).

<sup>3</sup>M. Lebrun, C. J. Martoff, U. Straumann, P. Truöl, C. Joseph, J. P. Perroud, M. T. Tran, J. Bistirlich, K. Crowe, J. Deutsch, G. Gregoire, R. Prieels, W. Dahme, and H. Baer, in *Proceedings of the Conference on Spin-Excitations in Nuclei, Telluride, Colorado, 1982* (Plenum, New York, to be published).

<sup>4</sup>M. Gmitro, H. R. Kissener, P. Truöl, and R. A. Eramzhyan, *Fiz. Elem. Chastits At. Yadra* **13**, 1230 (1982) [*Sov. J. Part. Nucl.* **13**, 6 (1982)].

<sup>5</sup>J. A. Bistirlich, K. M. Crowe, A. S. L. Parsons, P. Sharek, and P. Truöl, *Phys. Rev. Lett.* **25**, 689 (1970).

<sup>6</sup>A. Perrenoud *et al.*, Université de Lausanne report, 1981.

<sup>7</sup>H. R. Kissener and R. A. Eramzhyan, *Nucl. Phys.* **A326**, 289 (1979).

<sup>8</sup>G. C. Ball, G. J. Costa, W. G. Davies, J. S. Foster, J. C. Hardy, and A. B. McDonald, *Phys. Rev. Lett.* **31**, 395 (1973).

<sup>9</sup>J. Meyer-ter Vehn, *Phys. Rep.* **74**, 323 (1981).

<sup>10</sup>J. Speth, V. Klemm, J. Wambach, and G. E. Brown, *Nucl. Phys.* **A343**, 382 (1980).

<sup>11</sup>T. Suzuki, S. Krewald, and J. Speth, *Phys. Lett.* **107B**, 9 (1981).

<sup>12</sup>G. Strassner, P. Truöl, J. C. Alder, B. Gabioud, C. Joseph, J. F. Loude, N. Morel, A. Perrenoud, J. P. Perroud, M. T. Tran, E. Winkelmann, W. Dahme, H.

Panke, D. Renker, and H. A. Medicus, *Phys. Rev. C* **20**, 248 (1979).

<sup>13</sup>C. J. Martoff, J. A. Bistirlich, K. M. Crowe, M. Koike, J. P. Miller, S. S. Rosenblum, W. A. Zajc, H. W. Baer, A. H. Wapstra, G. Strassner, and P. Truöl, *Phys. Rev. Lett.* **46**, 891 (1981).

<sup>14</sup>D. B. Holtkamp, S. J. Seestrom-Morris, S. Chakravarti, D. Dehnhard, H. W. Baer, C. L. Morris, S. J. Greene, and C. J. Harvey, *Phys. Rev. Lett.* **47**, 216 (1981).

<sup>15</sup>M. A. Plum, R. A. Lindgren, R. S. Hicks, R. L. Huffman, G. A. Peterson, J. Lichtenstadt, M. A. Moinester, J. Alster, and H. Baer, *Bull. Am. Phys. Soc.* **27**, 530 (1982); and (unpublished).

<sup>16</sup>F. J. Kline, H. Crannell, J. M. Finn, P. L. Hallowell, J. T. O'Brien, C. W. Werntz, S. P. Fivozinsky, J. W. Lightbody, and S. Denner, *Nuovo Cimento* **23**, 137 (1974).

<sup>17</sup>The assays of the  $^{14}\text{C}$ - $^{12}\text{C}$  powder were performed at Oak Ridge National Laboratory.

<sup>18</sup>J. C. Alder, B. Gabioud, C. Joseph, J. F. Loude, N. Morel, A. Perrenoud, J. P. Perroud, M. T. Tran, B. Vaucher, E. Winkelmann, D. Renker, H. Schmitt, C. Zupancic, H. von Fellenberg, A. Frischknecht, F. Hoop, G. Strassner, and P. Truöl, *Nucl. Instrum. Methods* **160**, 93 (1979).

<sup>19</sup>J. A. Bistirlich, K. M. Crowe, A. S. L. Parsons, P. Skarek, and P. Truöl, *Phys. Rev. C* **5**, 1867 (1972).

<sup>20</sup>H. Ohtsubo, T. Nishiyama, and M. Kawaguchi, *Nucl. Phys.* **A224**, 164 (1974).

<sup>21</sup>N. Ohtsuka and H. Ohtsubo, *Nucl. Phys.* **A306**, 513 (1978).

<sup>22</sup>J. B. Flanz, dissertation, University of Massachusetts, Amherst, 1979 (unpublished); R. Hicks, private communication.

<sup>23</sup>K. Min, E. J. Winhold, K. Shoda, H. Tsubota, H.

- Ohashi, and M. Yamazaki, Phys. Rev. Lett. 44, 1384 (1980).
- <sup>24</sup>K. Min, E. J. Winhold, K. Shoda, H. Tsubota, M. Yamazaki, and M. Torikoshi, Bull. Am. Phys. Soc. 27, 719 (1982).
- <sup>25</sup>R. S. Hicks, R. A. Lindgren, B. Parker, G. A. Peterson, H. Thiessen, H. Crannell, and D. Sober, in Workshop on Nuclear Structure with Intermediate-Energy Probes, (Los Alamos National Laboratory Report LA-8303-C), 1980, p. 292; R. Hicks, private communication.
- <sup>26</sup>C. J. Martoff, J. A. Bistirlich, C. W. Clawson, K. M. Crowe, K. Koike, J. D. Miller, S. S. Rosenblum, W. A. Zaic, H. W. Baer, A. H. Wapstra, G. Strassner, and P. Truöl, Phys. Rev. C 27, 1621 (1983).
- <sup>27</sup>C. L. Morris, in Workshop on Nuclear Structure with Intermediate-Energy Probes, Los Alamos National Laboratory Report LA-8303-C, 1980, p. 57; C. Morris, private communication.
- <sup>28</sup>T. W. Donnelly, Phys. Rev. C 1, 883 (1970).
- <sup>29</sup>N. Ohtsuka, thesis, Osaka University, 1978; see also Refs. 21 and 22.
- <sup>30</sup>A. Perrenoud, thesis, University of Lausanne, 1979; see also Ref. 6.
- <sup>31</sup>T. de Forest and D. Walecka, Adv. Phys. 15, 1 (1966).
- <sup>32</sup>C. A. Fry, G. A. Beer, G. R. Mason, R. M. Pearce, P. R. Poffenberger, C. I. Sayre, A. Olin, and J. A. MacDonald, Nucl. Phys. A375, 325 (1982).
- <sup>33</sup>D. J. Millener and D. Kurath, Nucl. Phys. A255, 315 (1975).
- <sup>34</sup>S. Cohen and D. Kurath, Nucl. Phys. 73, 1 (1965).
- <sup>35</sup>H. U. Jäger and M. Kirchbach, Nucl. Phys. A291, 52 (1975).